Title	Wavelength dependence of photoreduction of Ag+ ions in glasses through the multiphoton process
Author(s)	Kondo, Yuki; Inouye, Hideyuki; Fujiwara, Seiji; Suzuki, Tishio; Mitsuyu, Tsuneo; Yoko, Toshinobu; Hirao, Kazuyuki
Citation	JOURNAL OF APPLIED PHYSICS (2000), 88(3): 1244-1250
Issue Date	2000-08-01
URL	http://hdl.handle.net/2433/39694
Right	Copyright 2000 American Institute of Physics. This article may be downloaded for personal use only. Any other use requires prior permission of the author and the American Institute of Physics.
Type	Journal Article
Textversion	publisher

Wavelength dependence of photoreduction of Ag^+ ions in glasses through the multiphoton process

Yuki Kondo,[a] Hideyuki Inouye, Seiji Fujiwara, Toshio Suzuki, and Tsuneo Mitsuyu
Hirao Active Glass Project, Exploratory Research for Advanced Technolog, Japan Science and Technology Corporation, Keihanna-plaza, Super-Lab 2F6, Seika, Kyoto 619-0237, Japan

Toshinobu Yoko
Institute for Chemical Research, Kyoto University, Uji, Kyoto 611-0011, Japan

Kazuyuki Hirao
Graduate School of Engineering, Kyoto University, Sakyo, Kyoto 606-8501, Japan

(Received 12 August 1999; accepted for publication 3 May 2000)

We have investigated the wavelength dependence of the photoreduction of Ag^+ ions in glass irradiated by visible femtosecond pulses. These pulses, issued at wavelengths ranging from 400 to 800 nm, were nonresonant with the glass absorption. In this article, a relationship between threshold powers, wavelengths, and linear and nonlinear refractive indices is described. The nonlinear refractive index of Ag^+-doped glass was measured by an optical Kerr shutter method. The wavelength dependence of threshold powers of the photoreduction is explained by considering linear and nonlinear refractive indices. The mechanism of the photoreduction is also discussed. © *2000 American Institute of Physics.* [S0021-8979(00)05615-2]

I. INTRODUCTION

Glasses are of great use in various industrial fields. As compared with other materials, glasses have various advantages in their thermal stability, chemical durability, hardness, transparency, etc. To date, the irradiation of light with a shorter wavelength such as ultraviolet light or X ray on glasses, has been utilized to change their surface structure through the photochemical reactions. For example, such an irradiation results in the reaction of the entire exposed region of the glass surface. However, since glass materials absorb the light with a shorter wavelength, the light intensity decreases as the light penetrates deeper into materials. Therefore, the reaction degree in the inside of glass materials is less than that at the surface. For the reason described above, a shorter wavelength light is adequate to modify the glass surface but not for the glass interior. However, there have been some studies using multiphoton processes. This multiphoton process caused by the femtosecond laser pulses having a high intensity is very attractive, since the light at a longer wavelength, for example visible light, can concentrate on the focal point inside the glasses without the absorption of the light. Namely, the feature of multiphoton reaction is a point access to a specific position inside glasses. Therefore, the multiphoton process is very useful in modifying the glass interior. It is well known that the electric field of one pulse of a focused femtosecond laser beam can be as high as 10^8-10^9 V/cm (light intensities of about 100 TW/cm^2). Therefore, when a 100 fs pulse with a 1 mJ pulse energy is focused onto an area of 10^{-4} cm^2, it may be possible to cause photochemical reaction through the multiphoton process. These photochemical reactions may occur even at visible wavelengths which are nonresonant with the glass absorption. From this viewpoint, it can be determined that the use of the femtosecond laser may become one of the newer tools to change the material's internal structure. More recently, the internal modification of glass structure has been reported using focused irradiation of ultrashort pulse lasers.[1–8] So far, we have reported on the photoreduction of Ag^+ ions to Ag atoms[8] with the focused irradiation of visible femtosecond pulses.[9–12] Focused irradiation of femtosecond pulses causes the following reaction: Ag^+ + nonbridging oxygen in glass (NBO) $\rightarrow Ag^0 + NBO^+$.[11] Namely, Ag^+ ions are reduced to Ag^0 atoms and hole trap centers at NBO near Ag^+ ions are formed by focused irradiation of femtosecond pulses at nonresonant wavelength. Moreover, we have shown that the photoreduction of Ag^+ ions is closely correlated with filamentation of the femtosecond beam due to self focusing.[11] However, the photochemical reaction induced by nonresonant femtosecond pulses has not been clarified yet. In this study, we investigate the wavelength dependence of the photoreduction of Ag^+ ions and propose a mechanism of the photoreduction.

II. EXPERIMENT

A. Sample preparation

The batch composition of the glass was the same as in our previous studies,[9–11] i.e., $74SiO_2-5Al_2O_3-4ZnO-17Na_2O-8F$ in mol ratio including 47 ppm of Sb_2O_3, 42 ppm of SnO_2, and 8 ppm of Ag. Reagent grades of SiO_2, Al_2O_3, ZnO, Na_2CO_3, NaF, Sb_2O_5, SnO_2, and AgCl were used as the raw materials. A 400 g batch was melted at 1450 °C for 2 h with stirring in a Pt crucible in air in an electric furnace. The liquid was poured onto a stainless steel plate. Glass was annealed at 470 °C for 4 h. Samples were

[a]Author to whom correspondence should be addressed; electronic mail: ykondo@agc.co.jP

polished to a thickness of 2 mm. The band gap of the examined glass was estimated to be between 6 and 7 eV by using Kramers–Kronig analysis of a reflectance spectrum of similar composition glass ($1Na_2O–1CaO–5SiO_2$) in Ref. 13. Irradiation of light with a photon energy higher than the band-gap energy causes the photochemical reaction, $Ag^+ + NBO \rightarrow Ag^0 + NBO^+$.

B. Focused irradiation of femtosecond laser beam

Light sources for irradiation of the samples were three kinds of femtosecond lasers at visible wavelengths: a regeneratively amplified 800 nm Ti–sapphire laser, which emitted 1 mJ, 125±5 fs, 1 kHz mode-locked pulses, second harmonic generation (SHG) light of a regeneratively amplified Ti^{3+}: Al_2O_3 laser generated by BaB_2O_4 (BBO) crystal which emitted 40 μJ, 125±5 fs, 1 kHz mode-locked pulses at 400 nm, and an optical parametric amplifier (OPA) which emitted 10 μJ, 155±5 fs, 630 nm, 1 kHz mode-locked pulses by pumping with a regeneratively amplified 800 nm Ti–sapphire laser. The wavelengths of the laser beam were set at 400, 630, and 800 nm. Details of the irradiation setup are described in Ref. 11. The laser beam was focused into the glasses through a focusing lens of 50 mm focal length. No intrinsic absorption is observed in the visible region, i.e., 400–800 nm with absorption coefficients $<10^{-2}\,cm^{-1}$. The spot sizes at 400, 630, and 800 nm were 14, 26, and 33 μm, respectively.

We have confirmed that the photochemical reaction $Ag^+ + NBO \rightarrow Ag^0 + NBO^+$ was caused by focused irradiation of visible femtosecond pulses.[11] Because the photochemical reaction region was obscure after irradiation, development (heat treatment) was performed to make it clear where the photochemical reaction region was. According to Stookey,[14] it is certain that Ag colloids act as nuclei for crystallization. After development, crystallites are precipitated using Ag colloids as nuclei. To clarify the photoreduction region, the samples after irradiation were heated at 540 °C for 30 min and held at 100 °C for 3 h and then heated again at 580 °C for 30 min to precipitate crystallites. A 2000× microscope was used to determine whether crystallization occurred at a focal point. The crystallized region is dependent on the heat treatment time in the normal heterogeneous/homogeneous crystallization process (nucleation and crystal growth). On the other hand, in this case, the crystallized region when heat treated at 580 °C for 30 min was the same as that for 10 h. This result shows that crystallization occurred using Ag colloids formed by a photochemical reaction induced by focused irradiation of femtosecond pulses. In addition, we confirmed that Ag-free glass showed no crystallization in the exposed region after heat treatment following irradiation of femtosecond pulses.[11] It can be said that the crystallized region coincides with the region where the photoreduction of Ag^+ ions to Ag atoms takes place. Therefore, in order to determine the extent of the photoreduction of Ag^+ ions, we measured the extent of crystallization by a 400× microscope.

When a laser beam with an ultrashort pulse such as femtosecond pulse is focused, light intensity I becomes high enough at the focal point to cause refractive index change given by the following equation:

$$n = n_0 + n_2 I. \tag{1}$$

Here n_0 is linear refractive index and n_2 is nonlinear refractive index. Self-focusing of the laser beam occurs due to an increase in refractive index caused by the high intensity I. On the other hand, formation of electron plasma due to the high electric field causes a decrease in the real part of the refractive index and self-defocusing of the beam occurs.[15–17] The balance between self-focusing, self-defocusing, and natural diffraction, makes a beam propagation without refraction and diffraction as if it propagates in an optical fiber. This phenomenon is called self-trapping or filamentation.[16–23] Therefore, filamentation due to self-focusing is closely related to nonlinear refractive index of glass n_2. Critical power of self-focusing P_{crit} is expressed by[23,24]

$$P_{crit} = \frac{3.77\lambda^2}{8\pi n_0 n_2}, \tag{2}$$

where λ is the wavelength. The value of P_{crit} is dependent on wavelength, linear, and nonlinear refractive indices. Linear and nonlinear refractive indices of glass are dependent on wavelength because of their dispersion. Therefore, measurements of linear and nonlinear refractive indices are very important to investigate the wavelength dependence on the threshold powers P_{thr} of the photoreduction of Ag^+ ions and to clarify the mechanism of photochemical reaction induced by nonresonant femtosecond pulses.

C. Measurement of linear refractive index

The linear refractive indices were measured with a variable angle spectroscopic ellipsometer (J. A. Woollam Co. Inc., V-VASE-DIRAR).

D. Measurement of nonlinear refractive index

Nonlinear refractive indices were measured by an optical Kerr shutter method. The configuration of the measurement is illustrated in Fig. 1. The light sources for the measurement were the lasers described in Sec. II B. The repetition rate was 1 kHz. We separated the laser beam into two parts: one was the gate beam and the other was the probe beam. The intensity ratio of the gate and the probe beam was 30:1. We focused the laser beams with diameters of 2 mm onto the glass sample by an achromatic lens with a focal length of 200 mm. The polarization angle of the gate beam was controlled by a half-wave plate. The glass sample was positioned between the polarizer and the analyzer in a cross-Nicol configuration set on the probe beam path. Detectors 1 and 2 were Si photodiodes with response times of 7 and 42 μs, respectively. Detector 2 was used as a reference. We measured the averaged probe signal transmitted through the analyzer delaying the gate beam against the probe beam by a computer-controlled stage. An aperture prevented the gate beam from entering detector 1. We measured the transmissivity T_1 for a cross-Nicol configuration and T_0 for an open-Nicol configuration. The extinction ratio of the linear polarization maintenance was over 30 dB.

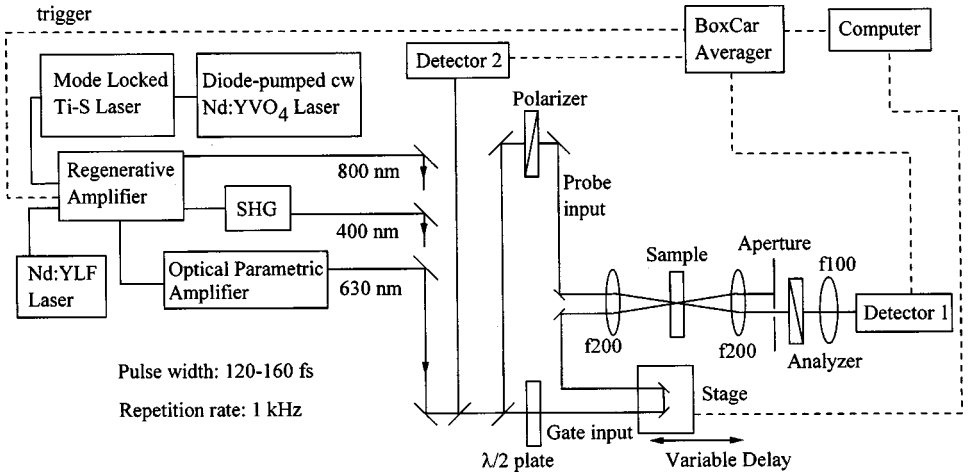

FIG. 1. The experimental setup for the Kerr shutter system. The principal light source for the gate beam is the regeneratively amplified Ti–sapphire laser. The SHG generator and an OPA are also used to generate the gate beam. The wavelengths of femtosecond laser beam were set at 400, 630, and 800 nm. The repetition rate was 1 kHz. We separated the laser beam into two parts: one is the gate beam and the other the probe beam. The intensity ratio of the gate and the probe beam was 30:1.

The refractive index change for the optical Kerr shutter configuration is given by the following equation:

$$n = n_0 + n_{2B(\mathrm{Kerr})} I_g , \tag{3}$$

where I_g is the gate intensity and $n_{2B(\mathrm{Kerr})}$ is the Kerr nonlinear refractive index (Kerr coefficient), which corresponds to the third-order nonlinear coefficient. The change in the refractive index here induces a shift in the phase ϕ of the probe beam. If the phase shift $\Delta\phi$ is small enough, using the angle θ_B between the linearly polarized gate and probe beams and $\Delta\phi$, the transmissivity T_1 for the probe beam is given by[25]

$$T_1 = T_0 \sin^2(2\theta_B)\sin^2\left(\frac{\Delta\phi}{2}\right) = T_0 \sin^2(2\theta_B)\left(\frac{\Delta\phi}{2}\right)^2 . \tag{4}$$

Using the change in the wave number of the probe beam Δk_p and the effective length of the sample L_{eff}, the $\Delta\phi$ is given by

$$\Delta\phi = \Delta k_p L_{\mathrm{eff}} = \frac{2\pi n_{2B(\mathrm{Kerr})} I_g}{\lambda_p} L_{\mathrm{eff}} . \tag{5}$$

Here, $L_{\mathrm{eff}} = [1-\exp(-\alpha L)]/\alpha$, α is the absorption coefficient and λ_p is the wavelength of the probe beam. The transmissivity T_1 shows a maximum at $\theta_B = \pi/4$ as expected by Eq. (4). Using the gate power $P_g = I_g/\pi a^2$ (a: beam radius at the focal point) instead of the gate intensity I_g and substituting Eq. (5) into Eq. (4), Eq. (4) is given by

$$\frac{T_1}{T_0} = \left(\frac{2 n_{2B(\mathrm{Kerr})} L_{\mathrm{eff}}}{a^2 \lambda_p}\right)^2 P_g^2 , \tag{6}$$

when $\Delta\phi$ is sufficiently small. When the transmissivity T_1 for the cross-Nicol configuration occurs due to the optical Kerr effect, T_1/T_0 is proportional to the square of P_g. From Eq. (6), the unknown Kerr coefficient $n_{2B(\mathrm{Kerr})}$ can be evaluated by comparing the T_1 value with the standard medium (in this case, SiO_2 glass) under the same gate power. The $n_{2B(\mathrm{Kerr})}$ value is represented by modifying the equation introduced by Kanbara[26] as follows:

$$n_{2B(\mathrm{Kerr})} = n_{2B,s(\mathrm{Kerr})} \frac{L_{\mathrm{eff},s}}{L_{\mathrm{eff}}} \left(\frac{(T_1/T_0)}{(T_1/T_0)_s}\right)^{1/2} , \tag{7}$$

where the suffix s indicates the standard, which was synthesized SiO_2 glass fabricated by the vapor axial deposition method (supplied by Asahi Glass Co. Ltd., Japan). The Δn in a Kerr shutter can be expressed by the following equation using the components, parallel ($\Delta n_{\parallel}$) and perpendicular ($\Delta n_{\perp}$) to the polarization of the gate beam

$$\Delta n = \Delta n_{\parallel} - \Delta n_{\perp} . \tag{8}$$

If the electronic polarization effect is dominant, $\Delta n_{\parallel} = 1/3 \Delta n_{\perp}$.[27] Therefore, Eq. (8) becomes as follows:

$$\Delta n = n_{2B} I_g = \tfrac{2}{3} \Delta n_{\parallel} . \tag{9}$$

When the wavelength of the gate beam is the same as that of the probe beam, $\Delta n_{\parallel} = n_2 I_g$. From Eq. (9), the nonlinear refractive index n_2 is given by

$$n_2 = \tfrac{3}{2} n_{2B(\mathrm{Kerr})} . \tag{10}$$

Substituting Eq. (10) into Eq. (7), the nonlinear refractive index of the glass sample was evaluated as follows:

$$n_2 = n_{2,s} \frac{L_{\mathrm{eff},s}}{L_{\mathrm{eff}}} \left(\frac{(T_1/T_0)}{(T_1/T_0)_s}\right)^{1/2} . \tag{11}$$

The value of $n_{2,s}$ of the synthesized SiO_2 glass as the standard sample is $2.48\times10^{-20}\,\mathrm{m^2/W}$ at 800 nm and $3.25\times10^{-20}\,\mathrm{m^2/W}$ at 400 nm.[28] We used the $n_{2,s}$ value of $2.88\times10^{-20}\,\mathrm{m^2/W}$ at 630 nm from Ref. 29. Although in Ref. 29, the value was measured at 694 nm, we assumed little dispersion from 630 to 694 nm. All glass samples were 1 mm in thickness.

To confirm that the electron polarization was the dominant mechanism for the nonlinear optical effect, we measured the decay of the probe transmittance at the cross-Nicol configuration by varying the time delay between gate and probe pulse. An autocorrelation trace of the gate pulse was also measured by using BBO crystal as the SHG crystal to estimate the pulse width of the gate beam.

III. RESULTS

A. Photochemical reaction

We investigated the dependence of the femtosecond laser power on the extent of the photochemical reaction region.

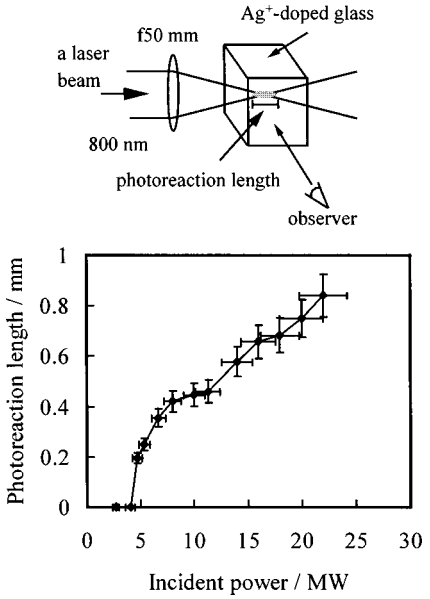

FIG. 2. Incident power dependence of the photoreduction region in the sample after 5000 pulses at 800 nm using a focusing lens of 50 mm focal length. An illustration shows the irradiation configuration. Here, the photoreduction region means the length of crystallites precipitated parallel to the direction of laser beam, which indicates the region where the reaction of $Ag^+ + NBO \rightarrow Ag^0 + NBO^+$ occurs.

Figure 2 shows the photochemical reaction length as a function of the incident power in a sample after 5000 pulses at 800 nm. An illustration shows the experimental scheme. Here, the photochemical reaction length means the length of the crystallites precipitated parallel to the direction of the laser beam, which indicates the reaction region of $Ag^+ + NBO \rightarrow Ag^0 + NBO^+$.[11] When the peak power defined as the pulse energy divided by the pulse width is more than 4 MW (about 0.4 TW/cm^2 in intensity), the photochemical reaction occurs and the reaction length increases with the increase of incident power. On the other hand, the photochemical reaction cannot occur if the peak power is less than 4 MW. We found that the reaction had a threshold in the incident power. It was possible to cause the photoreduction of Ag^+ ions at the focal point in the glass where the light intensity was sufficiently large. We observed the glass after irradiation of 5000 pulses and subsequent heat treatment. The incident power was varied stepwise by ND filters. We defined the experimental threshold power P_{thr} and intensity I_{thr} for the photochemical reaction at which the reaction began to occur. The threshold intensity I_{thr} is an intensity calculated on the assumption that the self-focusing does not occur and the beam size at the focal point is constant. Table I shows the values of P_{thr} and I_{thr}. It can be seen that the values of P_{thr} increase with increasing wavelength. This behavior is almost the same as that of the critical power P_{crit} of self-focusing vs λ.[23,24] The P_{thr} values at 630 and 400 nm are approximately 1/2 and 1/8 as compared with that at 800 nm, respectively. Threshold intensities I_{thr} are almost constant (about 0.4 TW/cm^2) within the experimental error and independent of wavelength.

TABLE I. Threshold powers and intensities of the photoreduction of Ag^+ ions at each wavelength of femtosecond pulses within errors of measurement.

Wavelength (nm)	P_{thr}(MW)	I_{thr}(TW/cm^2)
400	0.54±0.11	0.35±0.07
630	2.2±0.40	0.41±0.05
800	4.2±0.75	0.49±0.09

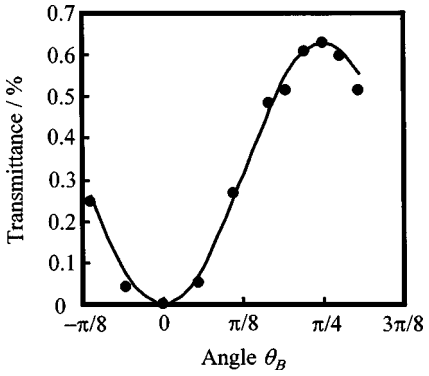

FIG. 3. Dependence of the probe transmittance T on the beam polarization angle θ_B. The laser wavelength was 800 nm. The solid line representing the calculated adequately coincides with the dots showing the observed results.

B. Measurement of nonlinear refractive index

From Eq. (4), the probe transmittance $T(=T_1/T_0)$ for the optical Kerr shutter is proportional to the square of $\sin(2\theta_B)$ as follows:

$$T \propto \sin^2(2\theta_B). \tag{12}$$

Figure 3 shows the dependence of the probe transmittance T on the angle θ_B between the linearly polarized gate and probe beams. The wavelength was 800 nm. The solid line represents the calculated curve. The observed T value shows a minimum at $\theta_B = 0$ and a maximum at $\theta_B = \pi/4$. The T values change as expected according to the relationship between the transmittance T and the angle θ_B between the linearly polarized gate and probe beams as given in Eq. (12). At other wavelengths, e.g., 400 or 630 nm also, the probe transmittance for the optical Kerr shutter showed the same dependence on the angle θ_B as that of 800 nm.

Figure 4 shows the probe transmittance as a function of the gate power at 800 nm. The result of SiO_2 glass is also shown in the figure as a reference. Below the gate power of 4 GW, the measured values of T increase in proportion to the square of P_g as expected from Eq. (6). When the power of a gate beam is the same, the Ag^+-doped glass shows about two times larger transmittance than that of SiO_2 glass.

To confirm that the electron polarization is the dominant mechanism for the nonlinear optical effect, we measured the decay of the probe transmittance at the cross-Nicol configuration by varying the time delay between the gate and probe pulses. An autocorrelation trace of the gate pulse was also measured by using BBO crystal as the SHG crystal. Figure 5 shows both the decay curve and the autocorrelation trace. The laser wavelength was 800 nm. It is clear that the Kerr shutter signal of the examined glass sample is detected only when the probe beam overlapped the gate beam. Hence, the

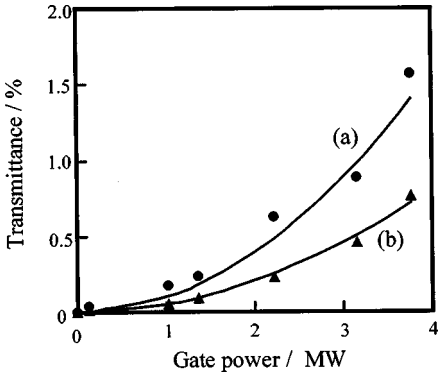

FIG. 4. Probe transmittance T measured at 800 nm as a function of the gate power P_g for: (a) Ag^+-doped glass and (b) SiO_2 glass as a reference. The T values of both glasses are proportional to the square of P_g.

response time of the Kerr signal of the sample is estimated to be below 150 fs, indicating that the Kerr signal of the sample originates from mainly pure electron polarization. Therefore, we can calculate n_2 values of Ag^+-doped glass by substituting the probe transmittance of standard SiO_2 glass and Ag^+-doped glass in Eq. (11). Table II shows n_2 values. Values of n_0 measured by the ellipsometer are also shown in Table II. Values of n_0 and n_2 increase with decreasing wavelength. This is due to the wavelength dispersion of the sample.

Figure 6 shows the experimental thresholds P_{thr} on a log–log plot as a function of normalized wavelength, $\lambda \cdot (n_0 \cdot n_2)^{-1/2}$, calculated by using values of n_0 and n_2 as shown in Table II. The relationship $P_{thr}=A\cdot(\lambda\cdot(n_0 \cdot n_2)^{-1/2})^C$, was used to fit the data, with correlation coefficient $C=2$. Here, A is constant. It is clearly seen that the experimental thresholds P_{thr} are proportional to the square of the normalized wavelength as in the case of the critical power for self-focusing, P_{crit}.

IV. DISCUSSION

As shown in Fig. 3, the observed T value changed according to the relationship given in Eq. (12), which indicates that the Kerr shutter operation using the Ag^+-doped glass is driven by the optical Kerr effect. If the thermal effect was the cause of the Kerr shutter operation, the probe transmittance T would not exhibit such a dependence on the θ_B value. The

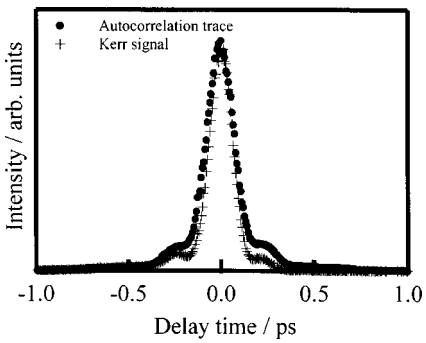

FIG. 5. Decay curve of the Kerr signal and the autocorrelation trace of the gate pulse at 800 nm. The autocorrelation trace was measured by using BBO crystal as SHG crystal.

TABLE II. Nonlinear refractive index measured by the optical Kerr shutter measurement and refractive index measured by the spectroscopic ellipsometer at each wavelength of femtosecond pulses.

Wavelength (nm)	n_2(cm^2/W)	n_0
400	8.1×10^{-16}	1.52
630	4.7×10^{-16}	1.51
800	3.5×10^{-16}	1.50

observed T value sufficiently coincides with the calculated one, which confirms that the nonlinear origin is the optical Kerr effect. We calculated n_2 values of Ag^+-doped glass by substituting the probe transmittance of the standard SiO_2 glass and that of Ag^+-doped glass in Eq. (11). We showed that the dominant mechanism of the Kerr effect was electron polarization considering the fact that the Kerr shutter response time was below 150 fs from Fig. 5. Therefore, it can be said that n_2 values are estimated with high accuracy.

We have shown that the photoreduction of Ag^+ ions is correlated with filamentation.[11] Filamentation due to self-focusing is closely related to linear and nonlinear refractive indices of glass. Critical power of self-focusing P_{crit} expressed by Eq. (2) is proportional to the square of the normalized wavelength obtained by linear and nonlinear refractive indices $\lambda\cdot(n_0\cdot n_2)^{-1/2}$.[23,24] In Fig. 6, it is clearly seen that the experimental threshold power of the photoreduction of Ag^+ ions P_{thr} is proportional to the square of the normalized wavelength $\lambda\cdot(n_0\cdot n_2)^{-1/2}$. This indicates that the photoreduction of Ag^+ ions is correlated with self-focusing. Generation of electric field high enough to cause self-focusing in the glass induces the photochemical reaction $Ag^+ + NBO \rightarrow Ag^0 + NBO^+$. Next, we will consider the possibility of some underlying mechanism of this reaction.

The Ag^+-doped glass sample has no absorption at the irradiated wavelengths, so the photoreduction of Ag^+ ions should be a multiphoton reduction process. In the case of a one-photon reaction, the photochemical reaction $Ag^+ + NBO \rightarrow Ag^0 + NBO^+$ occurs when irradiated with

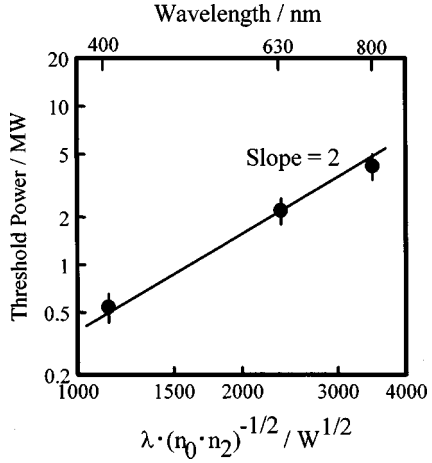

FIG. 6. Experimental thresholds P_{thr} plotted as a function of normalized wavelength $\lambda\cdot(n_0\cdot n_2)^{-1/2}$, calculated by using values of n_0 and n_2 shown in Table II. The data are fitted to the function $P_{thr}=A\cdot(\lambda\cdot(n_0\cdot n_2)^{-1/2})^C$, with correlation coefficient $C=2$.

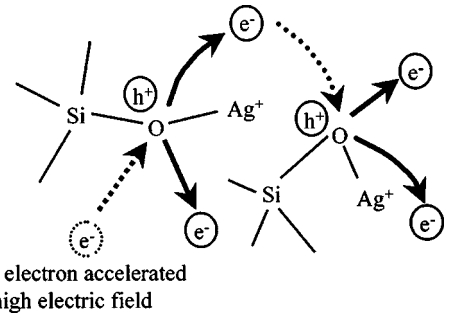

FIG. 7. Mechanism of the photochemical reaction of $Ag^+ + NBO \rightarrow Ag^0 + NBO^+$ in Ag^+-doped glass after focused irradiation of femtosecond pulses. In the first stage, the electron is excited by transitions from the valence band to the conduction band by multiphoton absorption. This free electron acts as an initiation for the photochemical reaction. After this free electron accelerated by high electric field interacts with NBO near Ag^+ ions, another free electron is formed and a hole is trapped at NBO. The new electron also accelerated by high electric field forms another free electron successively in the avalanche. Some of the free electrons combine with Ag^+ ions and Ag atoms are formed. This ionization process may continue until the exposure to femtosecond laser is stopped.

higher photon energy than the band gap of glass. The band gap of the examined glass is estimated to be between 6 and 7 eV. If multiphoton absorption is the main mechanism, as the irradiation wavelength approaches the energy corresponding to the band gap, the photochemical reaction due to multiphoton absorption should be easier and the threshold intensity should decrease. As seen in Table I, the threshold intensity appears to be essentially independent of the wavelength. This means that the multiphoton absorption is not the main mechanism. According to Bloembergen,[17] in the low frequencies, i.e., less than half the band gap, the threshold of nanosecond laser-induced electric breakdown is independent of frequency and the result is consistent with the avalanche ionization mechanism. In this study, the threshold intensities of the photochemical reaction are also independent of laser wavelength. We propose that the mechanism of the photochemical reaction $Ag^+ + NBO \rightarrow Ag^0 + NBO^+$ is also avalanche ionization. The mechanism we consider is as follows. Following the irradiation of the focused femtosecond laser, in the first stage, the electron is excited by transitions from the valence band to the conduction band by multiphoton absorption. This free electron acts as an initiation for the photochemical reaction. As soon as this electron is formed, the electron may be accelerated by the high electric field induced by the high peak power of femtosecond pulses. This accelerated free electron has a high possibility of reducing the Ag^+ ions and creating another new electron with a sufficiently high energy in the next collision. This ionization process may continue until the exposure to femtosecond laser is stopped. The illustration of the reaction is expressed in Fig. 7. Thus, free electrons are formed successively in the avalanche and holes are created in the glass and trapped by NBO near Ag^+ ions. If multiphoton absorption processes were important, they should be clearly observable in the difference of threshold intensity. However, the experimental threshold intensities are independent of laser wavelength. Therefore, high electric field (not high photon energy) is important for causing the photochemical reaction by nonresonant femtosecond pulses and multiphoton absorption is not the main mechanism. According to Bloembergen,[17] electron collision time is 10^{-14}–10^{-15} s. Avalanche ionization occurs in a time region less than those described above. Therefore, the electron can be accelerated at least in that time. In this study, we use laser pulses with a pulse width of subpicosecond. Although the pulse width is short as compared with that used by Bloembergen,[17] it can be assumed that the electron is sufficiently accelerated to cause avalanche ionization.

V. CONCLUSION

We have investigated the wavelength dependence of the photoreduction of Ag^+ ions caused by focused irradiation of visible femtosecond pulses nonresonant with the glass absorption. It was clearly seen that experimental thresholds P_{thr} were proportional to the square of the normalized wavelength $\lambda \cdot (n_0 \cdot n_2)^{-1/2}$ as in the case of the critical power for self-focusing P_{crit} vs the normalized wavelength behavior. The fact that the values of P_{thr} are proportional to the square of the normalized wavelength indicates that the photoreduction of Ag^+ ions is correlated with self-focusing. Generation of a high enough electric field to cause self-focusing in the glass induces the photochemical reaction $Ag^+ + NBO \rightarrow Ag^0 + NBO^+$. We propose avalanche ionization due to the high electric field of the femtosecond pulses as a mechanism because the threshold intensities I_{thr} of the photochemical reaction are independent of laser wavelength. From this study, it is clear that the high electric field due to high peak power of femtosecond pulses is important to cause the photoreduction of Ag^+ ions.

ACKNOWLEDGMENTS

The authors appreciate helpful discussions with Dr. Kenzo Miyazaki, Dr. Koichiro Tanaka, and Dr. Junpei Azuma of Kyoto University, and Dr. See L. Chin of Laval University in Canada. The authors are also grateful to Hirohisa Kanabara for his helpful advice in the optical Kerr shutter measurement.

[1] E. N. Glezer and E. Mazur, Appl. Phys. Lett. **71**, 882 (1997).
[2] D. Ashkenasi, H. Varel, A. Rosenfeld, S. Henz, J. Herrmann, and E. E. B. Cambell, Appl. Phys. Lett. **72**, 1442 (1998).
[3] S. Cho, H. Kumagai, I. Yokota, K. Midorikawa, and M. Obara, Jpn. J. Appl. Phys., Part 2 **37**, L737 (1998).
[4] J. Qiu, K. Miura, and K. Hirao, Jpn. J. Appl. Phys., Part 1 **37**, 2263 (1998).
[5] K. M. Davis, K. Miura, N. Sugimoto, and K. Hirao, Opt. Lett. **21**, 1729 (1996).
[6] Y. Kondo, K. Nouchi, T. Mitsuyu, M. Watanabe, P. G. Kazansky, and K. Hirao, Opt. Lett. **24**, 646 (1999).
[7] O. M. Efimov, K. Gabel, S. V. Garnov, L. B. Glebov, S. Grantham, M. Richardson, and M. J. Soileau, J. Opt. Soc. Am. B **15**, 193 (1998).
[8] L. B. Glebov, C. Depriest, O. M. Efimov, S. Grantham, and M. Richardson, Proceedings of XVIII Int. Congress on Glass, San Francisco, CA, 1998, p.17.
[9] Y. Kondo, T. Suzuki, H. Inouye, K. Miura, T. Mitsuyu, and K. Hirao, Jpn. J. Appl. Phys., Part 2 **37**, L94 (1998).
[10] Y. Kondo, T. Suzuki, H. Inouye, K. Miura, T. Mitsuyu, and K. Hirao, Proceedings of XVIII Int. Congress on Glass, San Francisco, CA, 1998, p.36
[11] Y. Kondo, K. Miura, T. Suzuki, H. Inouye, T. Mitsuyu, and K. Hirao, J. Non-Cryst. Solids **253**, 143 (1999).

[12] Y. Kondo, J. Qiu, T. Mitsuyu, K. Hirao, and T. Yoko, Jpn. J. Appl. Phys., Part 2 **38**, L1146 (1999).
[13] G. H. Sigel, J. Phys. Chem. Solids **32**, 2373 (1971).
[14] S. D. Stookey, Ind. Eng. Chem. **41**, 856 (1949).
[15] P. Monot, T. Auguste, L. A. Lompre, G. Mainfray, and C. Manus, J. Opt. Soc. Am. B **9**, 1579 (1992).
[16] N. Bloembergen, Opt. Commun. **8**, 285 (1973).
[17] N. Bloembergen, IEEE J. Quantum Electron. **QE-10**, 375 (1974).
[18] R. R. Alfano and S. L. Shapiro, Phys. Rev. Lett. **24**, 592 (1970).
[19] I. Golub, Opt. Lett. **15**, 305 (1990).
[20] Q. Xing, K. M. Yoo, and R. R. Alfano, Appl. Opt. **32**, 2087 (1993).
[21] A. Braun, G. Korn, X. Liu, D. Du, J. Squier, and G. Mourou, Opt. Lett. **20**, 73 (1995).
[22] O. G. Kosareva, V. P. Kandidov, A. Brodeur, C. Y. Chien, and S. L. Chin, Opt. Lett. **22**, 1332 (1997).
[23] A. Brodeur, F. A. Iikov, and S. L. Chin, Opt. Commun. **129**, 193 (1996).
[24] J. H. Marburger, *Progress in Quantum Electron* (Pergamon, Oxford, 1975), Vol. 4, p. 35.
[25] H. Kobayashi, H. Kanbara, M. Koga, and K. Kubodera, J. Appl. Phys. **74**, 3683 (1993).
[26] H. Kanbara, N. Sugimoto, S. Fujiwara, and K. Hirao, Opt. Commun. **148**, 101 (1998).
[27] D. H. Close, C. R. Giuliano, R. W. Hellwarth, L. D. Hess, F. J. Mcclung, and W. G. Wagner, IEEE J. Quantum Electron. **QE-2**, 553 (1966).
[28] A. J. Taylor, Opt. Lett. **21**, 1812 (1996).
[29] A. Owyoung, IEEE J. Quantum Electron. **9**, 1064 (1973).